Effect of Iron Catalyst on the Synthesis of Fullerenes and Carbon Nanotubes in Induction Plasma

G. Cota-Sanchez,[†,‡] G. Soucy,[*,†] A. Huczko,[§] J. Beauvais,[⊥] and D. Drouin[⊥]

Department of Chemical Engineering, Université de Sherbrooke, Blvd. de l'Université, Sherbrooke, J1K 2R1, Canada, Instituto Nacional de Investigaciones Nucleares, Salazar, Edo Mex., Mexico, Department of Chemistry, Warsaw University, Pasteura 1, 02-093 Warsaw, Poland, and Department of Electrical and Computer Engineering, Université de Sherbrooke, Sherbrooke, J1K 2R1, Canada

Received: June 1, 2004; In Final Form: September 24, 2004

The continuous synthesis of fullerenes and carbon nanotubes (CNTs) in induction plasmas at the 40-kW plate power level has been studied. Kinetics calculations were conducted to predict the conditions for fullerenes formation at the high plasma temperatures. "Carbon black-iron" powder mixtures were used as starting materials. The effects of the carbon−iron molar ratio and the reactant's feeding rates on the yield of fullerenes and CNTs were studied. The experimental results show that the synthesis of fullerenes and CNTs is clearly enhanced by the 4 mol % of Fe, present in the starting mixture, when it is fed at the low rate of about 1 g/min. Under these conditions, high yields of CNTs and C_{60} content, equal to 7.4 wt % of the total reaction product collected, were obtained.

1. Introduction

Several methods have been proposed to date for producing fullerenes and CNTs.[1−4] Among these, the methods of graphite laser ablation and vaporization by arc plasma have been the most successful. However, production rates for these batch reaction techniques still remain too small for the purposes of scale-up and commercialization. Thus, new methods for the continuous production of nanocarbons are being urgently sought. New synthesis systems, based on the use of dc plasma torches, have been developed recently.[5−7] The radio frequency (rf) plasma approach is also emerging as one of the most promising technologies for application to the production of fullerenes and CNTs in a continuous process regime, because of its remarkable properties such as the high temperature and the associated activated species density values available. To date, several attempts to use the rf plasma for the production of fullerenes have already been made. Thus, Peters and Jansen[8,9] have used a high-frequency (400 Hz) helium plasma reactor for this purpose, operated at the conditions of 30 kW power and under a medium He pressure (15 kPa). Various solid carbons were tested as the C raw material and the C_{60} content in the resulting "soot" product was reported as generally lying between 10 and 18 wt %. Yoshie et al.[10] used a hybrid plasma system consisting of a dc arc jet (5 kW) and a rf plasma (20 kW). Synthesis tests were carried out with argon as the plasma gas, at pressures of between 30 and 100 kPa. Carbon black, benzene, and acetylene were all used as the source of reactive carbon. A fullerene yield of about 7% was again obtained when a carbon black powder, fed at 0.5 g/min, was used as the starting material. The reactor pressure was reported to play a key role in the optimization of fullerene formation. Wang et al.[11−13] have more recently studied the synthesis of fullerenes by the direct vaporization of carbon powder, using a 30-kW rf plasma. Si addition to the starting carbon mixture was found to have the effect of enhancing the formation of the product C_{60}. The productivity of this process for fullerenes production has not yet, however, been reported. Todorovic-Markovic et al.[14] also used the rf plasma reactor to study the synthesis of fullerenes. Graphite powder, with a mean particle size of between 1 and 2 μm, was vaporized at 27 kW plasma power and at atmospheric pressure. The highest C_{60} yield (about 4.1 wt %) was obtained at a feed rate equal to 156 g/h. Mass spectroscopy analyses showed that the higher molecular weight fullerenes, such as C_{70}, C_{78}, C_{82}, and C_{84}, were also successfully produced. A kinetic model predicted the strong influence of carbon vapor concentration and plasma temperature on the yield of the fullerenes. Although the rf plasma approach has been shown to be an effective method for the production of fullerenes, very few reports have been published to date on the synthesis of CNTs with this continuous process method.[15,16]

The particular work presented here is focused on the application of induction plasma for the continuous production of fullerenes and CNTs, and is accompanied by a preceding note on the theoretical considerations concerning the kinetics of this process.

2. Theoretical Background

Cota-Sanchez[16] has earlier reported on a thermodynamic study of the formation of fullerenes at high temperatures. It was shown in this study that the fullerene formation temperature range lies between 2250 and 3800 K, while the precursor species (C_2 and C_3 molecules) are formed at temperatures above 2500 K. The results have also shown that the formation of fullerene precursors and molecules is favored when pure carbon is used as starting material. The use of higher carbon feed rates and higher pressures also enhances the yield of fullerenes. However, the low equilibrium concentrations of fullerenes, as calculated during the study, indicate that the formation of fullerene

* Address correspondence to this author. E-mail: gervais.soucy@usherbrooke.ca. Phone: 819-821-7171. Fax: 819-821-7955.
† Department of Chemical Engineering, Université de Sherbrooke.
‡ Instituto Nacional de Investigaciones Nucleares.
§ Warsaw University,
⊥ Department of Electrical and Computer Engineering, Université de Sherbrooke.

10.1021/jp047629z CCC: $27.50
Published on Web 11/19/2004

molecules is not realized under the equilibrium conditions existing in the plasma.

In an attempt to predict more precisely the formation of fullerenes under thermal plasma conditions, a simple kinetic mechanism was developed to better understand the kinetic behavior of the carbon species involved in the reaction mechanism at temperatures above 2000 K.

The kinetic study of any reacting plasma system[17,18] provides information regarding the reaction rates of chemical species, the influence of the operating parameters on the reaction rates, and the detailed reaction mechanism.

It is clear that a complete kinetic study of the plasma chemical process for fullerenes formation should include homogeneous and heterogeneous catalytic chemical pathways for carbon particle growth. However, such a study is still not possible due to the lack of reliable data on reaction kinetics for the catalytic formation of fullerenes structures and of thermochemical data for all carbon species likely to be involved in the reacting system.

In addition, although a kinetic simulation capable of reproducing the experimental results would be outstanding, that simulation work is beyond the overall objective of the kinetic study of fullerenes formation. This study is only focused on the analysis of the evolution through time of both precursors species and fullerenes as a function of the initial carbon concentration, in the range of the optimal temperatures for the fullerenes formation obtained in the thermodynamic study.[16]

By correlating simulation and experimental results, it might be possible to draw overall conclusions regarding the performance of the reactor, such as the gas temperatures in which the growth of fullerenes is favored, and the reactor section in which these temperatures can be found.

According to Kee et al.,[19] the elementary reversible reactions I, involving K chemical species, can be generally represented by

$$\sum_{k=1}^{K} \nu'_{ki} \mathrm{X}_k \leftrightarrow \sum_{k=1}^{K} \nu''_{ki} \mathrm{X}_k \qquad (i = 1, ..., I) \tag{1}$$

where X_k is the chemical symbol for the kth species, and ν'_{ki} and ν''_{ki} are the forward and reverse stoichiometric reaction coefficients, respectively.

The mathematical model of this kinetic system produces K differential equations, which represent the production or consumption of the kth chemical species as a time function, according to the equation

$$\frac{\mathrm{d}[\mathrm{X}_k]}{\mathrm{d}t} = \sum_{i=1}^{I} \upsilon_{ki} \left\{ k_{\mathrm{f}i} \prod_{k=1}^{K} [\mathrm{X}_k]^{\nu'_{ki}} - k_{\mathrm{r}i} \prod_{k=1}^{K} [\mathrm{X}_k]^{\nu''_{ki}} \right\} \tag{2}$$

with

$$\upsilon_{ki} = \nu''_{ki} - \nu'_{ki} \tag{3}$$

where $[\mathrm{X}_k]$ is the molar concentration for the kth chemical species and $k_{\mathrm{f}i}$ and $k_{\mathrm{r}i}$ are the forward and reverse rate constants for the ith reaction, respectively.

The forward rate constants are assumed to have the Arrhenius temperature dependence, according to the equation

$$k_{\mathrm{f}i} = A_i T^{\beta_i} \exp\left(\frac{-E_i}{RT}\right) \tag{4}$$

where A_i is the preexponential factor, β_i the temperature exponent, and E_i the activation energy for the ith reaction. Here, k is expressed in cm^3/mol s, T in K, and E in kJ/mol.

The reverse rate constants are then calculated, using the formula

$$K_{\mathrm{c}i} = \frac{k_{\mathrm{f}i}}{k_{\mathrm{r}i}} \tag{5}$$

where K_{ci} is the equilibrium constant for the ith reaction.

The resulting kinetic system with K differential equations was resolved, using the Chemical Kinetic Simulator computer software, version 1.0.[20] This routine finds a solution using a stochastic simulation method,[21] in which changes in the system are modeled by randomly selecting a factor among the probability-weighted reaction steps.

2.1. Reaction Mechanism for the Growth of Planar Graphitic Structures and Fullerenes. A chemical kinetic study was performed to analyze the time evolution of fullerene precursors, fullerenes, and related planar graphitic structures, under thermal plasma conditions. The kinetic mechanism takes into consideration a consecutive reactions' scheme for the formation and growth of condensed carbon particles. The kinetic mechanism included the following steps: the vaporization of solid carbon, the formation of fullerene precursors such as C_2 and C_3, the growth of the carbon nuclei by the consecutive incorporation of C_2 and C_3 particles, and the transformation of the carbon nuclei to planar graphitic structures or to fullerenes. Table 1 shows the elementary reactions involved in the reaction mechanism and the kinetic parameters for the rate constants (k), according to the Arrhenius expression. For a given reaction, all relevant kinetic parameters were taken from the literature or were otherwise calculated, using equilibrium constant values.

Additionally, the kinetic parameters for the reaction $C_2 + C_2 = Cn$ were considered to be those of the reaction $C_2 + C_2 = C_4$, while the kinetic parameters for the reaction $C_3 + C_3 = C_6$ were used for the reaction $C_3 + C_3 = Cm$.

In the kinetic mechanism, [Cs] is the initial solid carbon concentration; [C] is the carbon gas concentration; [C_2] and [C_3] are the concentrations of precursor materials; [Cn] and [Cm] are the concentrations of the condensed carbon particles; [Sn] and [Sm] are the concentrations of planar graphitic soot; [Fn] and [Fm] are the concentrations of the fullerenes; and [M] is the concentration of the diluent-gas particles.

As can be seen from the table, the primary step involves the vaporization of Cs subsequently followed by the reactions to produce the active fragments, C, C_2, and C_3, which are all considered to be the building materials for planar graphitic structures and fullerenes. For simplicity, it is also assumed that the boundaries between the nuclei and the condensed carbon particles lie in the regions of C_4 and C_6 with the solid carbon particles, which are designated by the symbols Cn and Cm. Thus, Cn and Cm nuclei are considered to be the starting materials in the formation reactions of planar graphitic structures (Sn, Sm) and fullerenes (Fn, Fm). The formation reactions of the fullerene-like structures, Fn and Fm, involve a rate constant characterized by a sharp maximum at the average particle size of 70 carbon atoms.[23] Therefore, the Cn and Cm approximations only take into account the growth of the total weight of condensed carbon particles.

It is important to note that the kinetics mechanism assumes a spheroidal approximation for the carbon particle growth and, at the same time, the assumptions made with respect to chains and planar and closed molecules are implicitly considered only in the thermochemical data.

TABLE 1: Kinetic Parameters for the Reactions Involved in the Growth Mechanism of Fullerenes

reaction	A	β	E	ref
solid carbon vaporization				
$Cs = C$	3.70×10^5	0.0	73.7	22
C_2 precursor formation				
$C + C + M = C_2 + M$	3.10×10^7	−1.5	−460.2	23
$C + C = C_2$	5.20×10^{10}	−0.5	25.5	23
C_3 precursor formation				
$C_2 + C = C_3$	1.28×10^{13}	−1.24	2.4	23
$C_2 + C_2 = C_3 + C$	2.50×10^{14}	0.0	74.9	23
growth of the nuclei via C_2				
$C_2 + C_2 = Cn$	6.62×10^4	0.64	−135.7	23
$C_2 + Cn = Cn$	4.50×10^{12}	0.5	0.0	23
$C_2 + Cm = Cm$	4.50×10^{12}	0.5	0.0	23
growth of the nuclei via C_3				
$C_3 + C_3 = Cm$	3.16×10^4	0.0	−88.3	23
$C_3 + Cm = Cm$	4.50×10^{12}	0.5	0.0	23
$C_3 + Cn = Cn$	4.50×10^{12}	0.5	0.0	23
transformation of the nuclei into planar graphitic structures				
$Cn = Sn$	1.00×10^6	0.0	0.0	23
$Cm = Sm$	1.00×10^6	0.0	0.0	23
transformation of the nuclei into fullerenes				
$Cn = Fn$	3.00×10^{13}	0.0	300.0	23
$Cm = Fm$	3.00×10^{13}	0.0	300.0	23

TABLE 2: Formation Enthalpy (ΔH_f) and C_p Coefficients for That Species Involved in the Chemical Kinetics

specie	ΔH_f (kJ/mol)	a_1 (J/mol)	$10^4 a_2$ (J/mol K)	$10^7 a_3$ (J/mol K^2)	$10^{11} a_4$ (J/mol K^3)	ref
C	716.67	21.09	−7.69	4.50	−4.47	24
C_2	837.74	32.17	41.90	−5.32	3.84	24
C_3	820.06	31.80	170.00	−47.90	36.20	24
Cm	1225.91	152.91	−1745.00	1450.00	−3180.00	25
Cn	970.69	43.72	420.00	−134.00	135.00	24
Cs	1.89	5.51	201.00	−62.60	64.20	24
Fm	2755.00	357.79	14400.00	−4820.00	5080.00	26
Fn	2530.00	302.21	12300.00	−4120.00	4360.00	26
M	0.0	0.0	200000.00	0.0	0.0	24
Sm	716.67	21.09	−7.69	4.50	−4.47	24
Sn	716.67	21.09	−7.69	4.50	−4.47	24

Table 2 shows the thermochemical data as used during these computations, such as that required for the formation enthalpy (ΔH_f) at 298.15 K and for the specific heat (C_p) coefficients, which were expressed according to eq 6.

$$C_p = a_1 + a_2 T + a_3 T^2 + a_4 T^3 \tag{6}$$

The effects of these two operating parameters on the kinetic behavior of the reacting system were the next parameters to be studied. The first was the effect of the molar ratio between the solid carbon and the plasma gas. The second effect was related to the operating temperature. Three different simulations were performed at the selected constant temperatures of 2000, 2500, and 3000 K.

2.2. Effect of the Initial Molar Ratio of Solid Carbon−Neutral Gas on the Kinetics of the Reacting System. The initial molar ratios between the input solid carbon and the plasma gas (He) were varied. The goal here was to evaluate the influences of both high, inert plasma gas concentrations and high initial carbon concentrations on the chemical kinetics prevailing during fullerene molecular growth.

The kinetic behavior of the carbon species, when the reacting system is considered to be under the condition of high level dilution by the plasma gas, is depicted in Figure 1, while the behavior under high initial carbon concentration is shown in Figure 2. Solid carbon−inert gas molar ratios of 0.05 and 0.25, respectively, were used in these evaluations.

Figures 1 and 2 show that solid carbon vaporization is reached approximately 1×10^{-3} s after initiation, under both conditions. Variation of the initial conditions clearly affects the molar concentration of the C, C_2, and C_3 species, the fullerenes (Fn), and the planar graphitic structures (Sn), as produced via the C_2 precursors.

The reaction rate for C compound formation is accelerated when a high solid carbon concentration value is used as the starting condition. For example, when a high solid carbon concentration is used, C compound formation begins at about 1×10^{-9} s instead of at 1×10^{-8} s for the high inert gas dilution condition. As a result, C_2, Sn, and Fn concentrations are also increased and their respective reaction rates are also accelerated. Fullerene and graphitic structures formation, via the C_2 precursor, is also obviously enhanced under these initial high carbon concentration conditions.

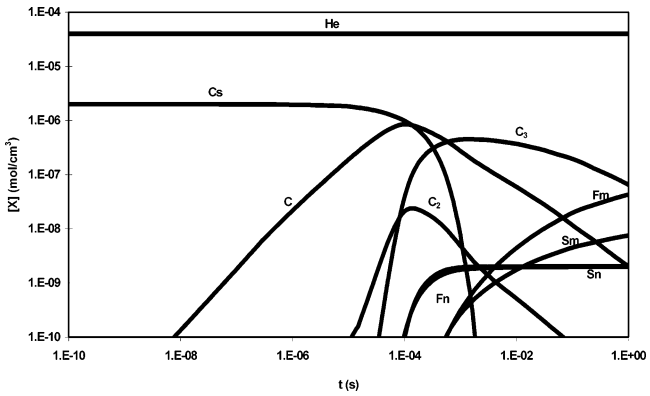

Figure 1. Chemical kinetics for various carbon species during fullerenes growth under high dilution conditions: 2×10^{-6} mol Cs + 4×10^{-5} mol He, $T = 2500$ K.

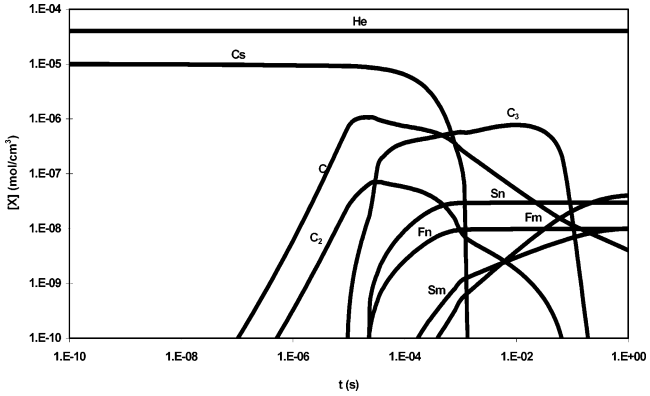

Figure 2. Chemical kinetics of carbon species during fullerenes growth at high solid carbon concentration: 1×10^{-5} mol Cs + 4×10^{-5} mol He, $T = 2500$ K.

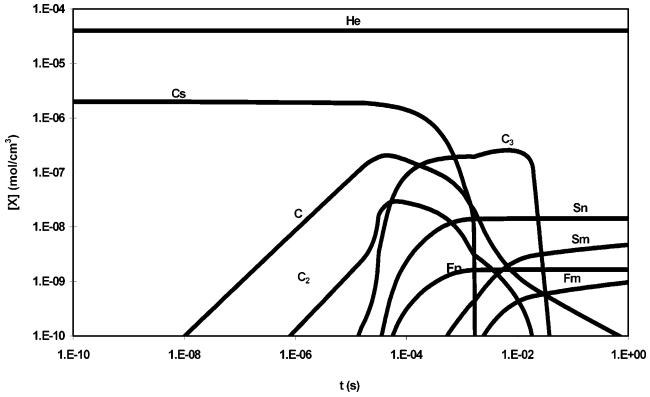

Figure 3. Chemical kinetics of carbon species during fullerenes growth at a temperature of 2000 K: 2×10^{-6} mol Cs + 4×10^{-5} mol He.

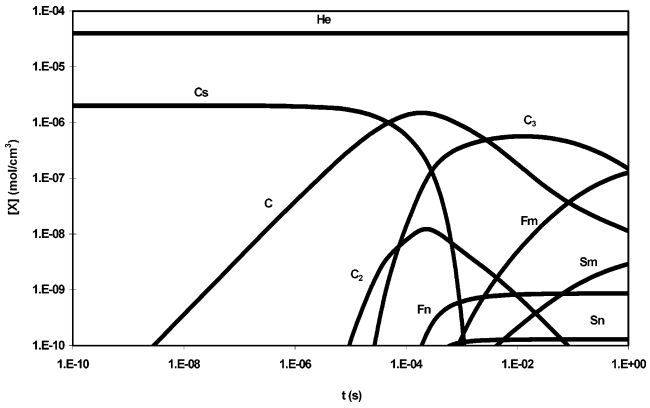

Figure 4. Chemical kinetics of carbon species during fullerenes growth at a temperature of 3000 K: 2×10^{-6} mol Cs + 4×10^{-5} mol He.

2.3. Effects of Temperature on the Kinetics of the Reacting System. Three simulations at different temperatures were performed to determine the effects of temperature on the reacting system kinetics. Figure 2 shows the simulation results with a reaction temperature of 2500 K, while Figures 3 and 4 present the simulation results at 2000 and 3000 K, respectively. A comparison of the results of these calculations shows that higher reaction temperatures clearly accelerate the reaction rate. The C compound formation begins at about 1×10^{-8} s for 2000 K (Figure 3), about 8×10^{-9} s for 2500 K (Figure 2), and 6×10^{-9} s for 3000 K (Figure 4).

An increase in the reaction temperature strongly enhances the formation of the carbon species, C and C_3. These species in turn favor fullerene formation (Fm), via the sequential additions

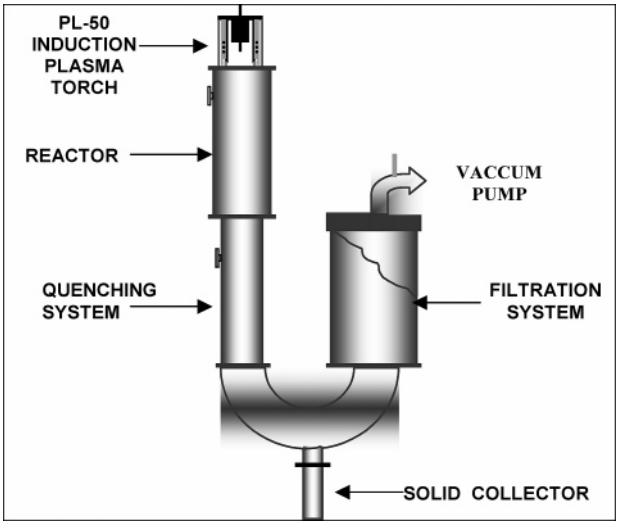

Figure 5. Experimental setup for the synthesis of fullerenes and nanotubes.

of C_3 precursors. The molar concentration of the C_2 species remains almost unaffected, despite the increasing reaction temperature. As a result, the fullerene concentration (Fn), produced via the sequential addition of C_2 precursors, is only slightly lower.

The increase of reaction temperature has a remarkable effect on the formation of planar graphitic structures, via the addition of C_2 and C_3 precursors. At higher temperatures, the concentration of graphitic structures (Sn and Sm) tends to decrease and the preferential formation of amorphous rather than graphitic carbon is predicted.

These results show that the use of high reaction temperatures favors the fullerene formation reaction and limits the formation of graphitic structures. However, it is important to remember that under these conditions, the formation of C_2 and C_3 species is also favored. As a consequence, a high yield of amorphous carbon can also be expected.

It is important to note that the concentrations of C, C_2, and C_3 species agree with those estimated by the thermodynamic equilibrium computations[16] over the range of temperatures used in the kinetic study.

3. Experimental Setup and Procedures

The experimental equipment setup, separated into two sections for practical and technical purposes, is shown in Figure 5. Section one included the rf induction plasma torch (a Tekna PL-50 induction plasma unit, with a ceramic confinement tube of 50-mm i.d. and a 5-turn coil), the reactor, and the quenching zone. The stainless steel reactor and the quenching tube were constructed with water-cooled jackets for carbon vapor condensation. A Lepel 60-kW generator, providing an oscillator frequency of 2 to 5 MHz, was used as the rf power supply. The second section included the product filtration system, comprised of three stainless steel filters to separate the fullerene "soot" before the conveying gas was drawn off by the vacuum pump. This section also comprised a blow back connection for filter cleaning and for allowing continuous operation of the reactor. The flow rates of the plasma gases were maintained constant, as shown in Table 3, presenting the plasma operational parameters.

A series of experimental tests were initially performed to evaluate the influence of the iron catalyst on the formation of fullerenes and CNTs. Carbon black powder from Cabot, Inc.

TABLE 3: Operating Conditions Used during the Experimental Tests[a]

test no.	Fe content in CB−Fe mixture (mol %)	mixture feeding rate (g/min)	run time (min)	recovery (%)		C_{60} content (wt %)	
				1st section	2nd section	1st section	2nd section
1	0.0	0.6	10	60	40	0.2	1.6
2	0.0	2.0	15	61	39	0.1	0.5
3	2.0	0.4	14	76	24	1.8	6.8
4	2.0	2.1	15	85	15	1.0	5.6
5	4.0	0.9	13	70	30	3.5	7.4
6	4.0	2.1	10	75	25	2.2	6.4
7	8.0	0.8	15	69	31	0.9	2.8
8	8.0	2.1	15	78	22	0.6	1.9
9	15.0	0.5	15	76	24	1.6	3.9
10	15.0	1.8	13	71	29	0.3	0.6

[a] Constant parameters: powder gas flow rate, Ar, 8 slpm; central gas flow rate, Ar, 25 slpm; sheath gas flow rate, He, 120 slpm; reactor pressure, 66 kPa; plate power, 40 kW.

was used as the carbon source and iron powder (Fe, 99.8%, 10 $\pm$ 5 μm) was used as the catalyst. Both powders were mixed together at different molar ratios with use of a rotary mixer operated at 50 rpm over a 10-min period. The reactant mixture was axially fed into the plasma through a water-cooled probe, positioned at the center of the plasma torch, using a Sylco MARK IX (serial 579) powder feeder.

The solid particulates were vaporized in the plasma zone and a condensate generated the fullerene soot, which was later recovered from the water-cooled walls of the reactor, the quenching zone, and the filtration system. A 100-mg sample of the product soot was leached with 50 mL of toluene by using ultrasonic bath agitation for 10 min. After filtration, a wine-red/brown solution was analyzed, using UV/vis absorption spectroscopy at 329 nm for C_{60} determination. The morphology of the soot (higher fullerene structures and CNTs) was also studied with use of a Hitachi S4700 field emission electron microscope, operated at 1.5 kV, and a Hitachi H750 transmission electron microscope, operated at 125 kV.

4. Results and Discussion

According to the parametric study, previously presented elsewhere,[16] high plate powers, high system pressures, and low raw material feed rates all favor the synthesis of nanocarbons by means of induction plasma. Hence, in the present tests, the plate power and the system pressure were maintained constant, at 40 kW and 70 kPa, respectively. Iron content and reactant mixture feed rates were varied to study their effects on the synthesis of fullerenes and CNTs. Table 3 contains the experimental results in terms of the C_{60} yields and the mass percent recovered from the reactor and the filter sections. In all experimental tests, a very light, soot-like product was deposited on the reactor and filters walls, with about 70% of the produced fullerene soot being obtained from the first section of the plasma system.

The C_{60} yield results clearly show that both the feed rate and the Fe concentration in the powder mixture play key roles in the fullerenes synthesis. It is evident that higher C_{60} yields were synthesized when lower feed rates of raw materials were used. This result is in contrast to that obtained in the kinetics study. According to the kinetics, the formation of fullerenes should be enhanced at the higher initial carbon concentrations. This observation can be explained by taking into account the vaporization phenomena of the reactants, processes that are far from complete. Under higher feed rate conditions, the solid matter effectively quenches the plasma and higher energy amounts are required to vaporize the reactant particulates. Thus, the overall plasma temperature is decreased, and consequently, reactants gasification is incomplete. Under these conditions, the carbon vapor pressure inside the plasma tail is relatively low and the formation of C_2 and C_3 radicals, which are considered to be fullerene precursors, is further limited. For all tests performed in this series, the higher C_{60} contents were found in the products collected in the filter section. This result is evidently related to the longer reaction times (and thence to the higher degrees of vaporization achieved) of these reactants.

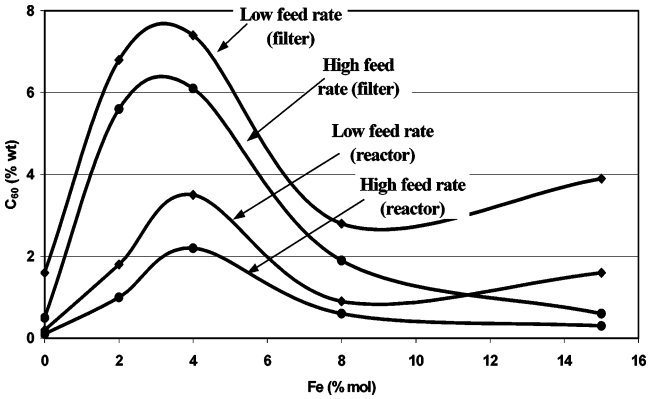

Figure 6. Effect of catalyst concentration on the C_{60} yield.

Figure 6 shows the results for C_{60} content found in the soot recovered from the reactor and filters, versus the iron concentration in the starting mixture. Higher C_{60} yields were obtained in all of those tests where the Fe catalyst was used, as compared with those obtained by pure carbon vaporization only (Tests 1 and 2). The highest C_{60} concentration (7.4 wt %) was synthesized when 4 mol % of Fe was used in the starting mixture.

Although the use of catalysts has earlier been shown to influence the yield of fullerenes,[11,16,27] their effects on the formation of fullerenes are still unclear. It is thought that a type of photocatalytic effect might influence the synthesis of fullerenes. It is well-known[28] that plasmas are intense sources of UV radiation and fullerenes are known to be highly sensitive to UV light.[29,30] Plasma radiation spectra in the presence of Fe vapors are both stronger and distinctly different in comparison to those of the pure carbon plasma. Thus, the yields of fullerenes might be enhanced in plasmas containing the metal vapors. Under these conditions, higher concentrations of C_2 and C_3 fullerene precursors might be produced. At the same time, the UV radiation might destroy some fullerene molecules, generating smaller fullerene fragments. These fragments may in turn act as growth sites for the polymerization of C_2 and C_3 precursors, producing new fullerene molecules in the reactor zones outside of the plasma zone where the UV radiation does not normally penetrate (particle filters section).

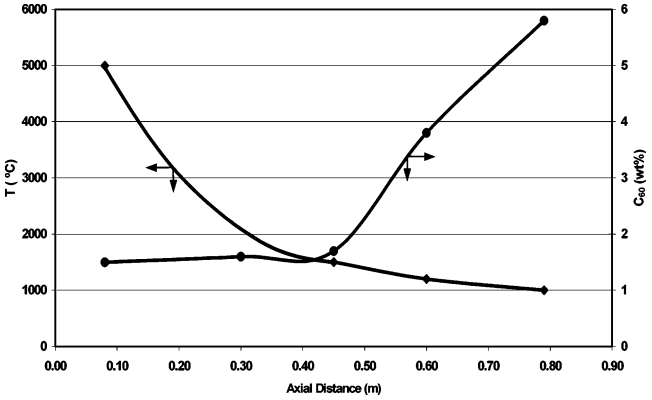

Figure 7. Gas temperature and C_{60} profiles along the reactor section (test no. 5).

A preliminary evaluation of the process kinetics was also conducted. Figure 7 shows the profiles of the reactor temperature and the C_{60} concentrations found in soot samples collected at various distances along the reactor length and the down stream quenching section, for Test No. 5.

While the highest temperature, about 5000 °C, was estimated by the optical emission associated with the Swan band, emitted by C_2 radicals,[16] gas temperatures at axial distances of 0.45, 0.60, and 0.80 m were measured, using a series of K-type thermocouples.

The results of the gas temperature and C_{60} concentration profiles show that higher C_{60} concentrations are found in the reactor zones where lower temperatures are present. Although these results are in contrast with those found in the kinetic study, in which higher temperatures favored the formation of fullerenes, this finding can be explained by taking into account that a formation−condensation phenomenon of fullerenes occurs along the reactor and the quenching length. That is, carbon particles are vaporized in the highest plasma temperatures (between 5000 and 8000 K), followed by, according to the kinetic study, the synthesis of fullerenes in the reactor zones (between 0.2 and 0.3 m) where temperatures of between 2000 and 3000 K predominate, and finally condensation in the cooler zones following the hot gas flow into the system. Furthermore, due to their nanometric size, fullerenes are more easily transported by the hot gas throughout the reactor length, as observed by the higher C_{60} yield (7.4 wt %) subsequently determined in the filter soot.

Taking into account an estimated average gas velocity of about 1.8 m/s,[16] the residence time of the reactive species was evaluated to be about 50 ms, in the reactor zones with temperatures ranging between 2000 and 3000 K.

Because the formation of fullerenes (Fn, Fm) begins in the range from 0.1 to 5 ms (see Figures 1, 3, and 4), it can be assumed that the growing molecules experience sufficient time exposure during their growth within the high-temperature gas zone. Thus the bonding rearrangement and "annealing" of the fullerene molecules are favored. These conditions increase the fraction of carbon species possessing the structure with the lowest binding energy and maximize the content of fullerenes in the soot collected at the reactor exit. In other words, the formation of fullerenes along the reactor and quenching sections is due to the temperature history and residence times of carbon clusters traversing the high-temperature environment. In fact, for all of the tests performed, higher concentrations of C_{60} were always found in the soot recovered from the filters, indicating that fullerenes are effectively formed following the flow of the hot gas throughout the plasma system. Therefore, it is reasonable

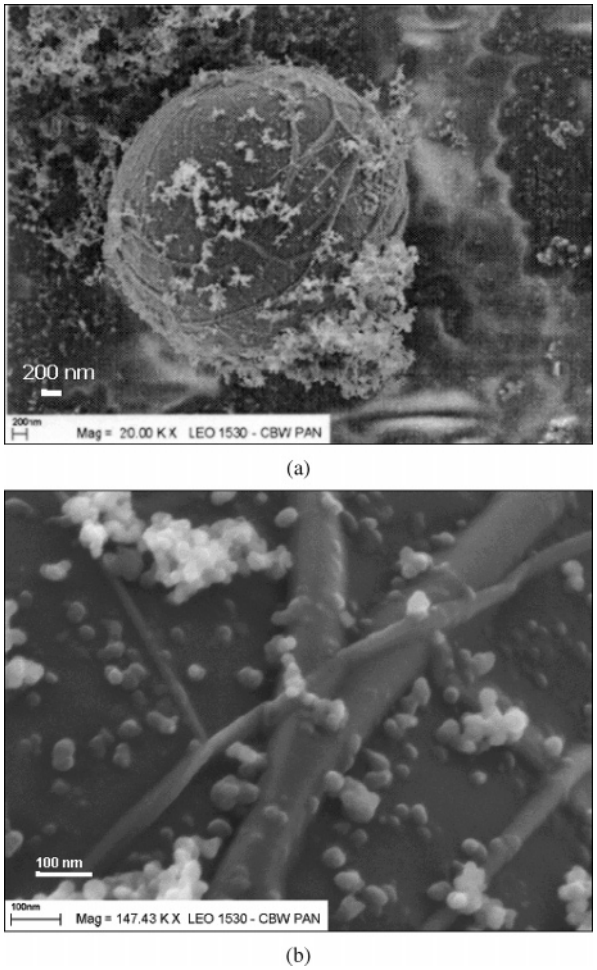

Figure 8. SEM micrographs of an unreacted metallic particle surrounded by carbon films produced in test no. 9.

to conclude that the growth kinetic mechanism, involving sequential additions of C_2 and C_3 fullerene precursors, strongly represents the carbon growth pattern of fullerenes taking place at high temperatures.

Figure 8a,b shows SEM micrographs of a specific type of carbon encapsulation found in the fullerene soot produced in Test No. 9. In this encapsulation, the unreacted catalyst particle is partially surrounded by carbon nano- and microparticles. This particle, which had survived the plasma conditions without evaporation, is covered with some "spaghetti-like" nanofibers. Interestingly, these figures show the superposition of carbon fibers, which may well be the result of some kind of carbon deposition phenomena. Carbon nanoparticles produced in the plasma tail are subjected to strong electric fields, large temperature gradients, and asymmetric absorption of incident radiation within the particle. These phenomena eventually enhance the migration and interaction of electrons, ions, and molecules.

The combined effect of the electric field, thermo- and photophoresis effects, might cause the migration, diffusion, and absorption of condensing carbon species onto the catalytically active particle surface. Then, these carbon species diffuse through the active sites of the particle surface and precipitate to form the carbon fiber body.

The migration of the remaining carbon species around the particle surface forms the fiber skin component. The nanofiber "spaghetti-like" configuration around the particle seems to be produced by the chaotic movement of the particle in the plasma

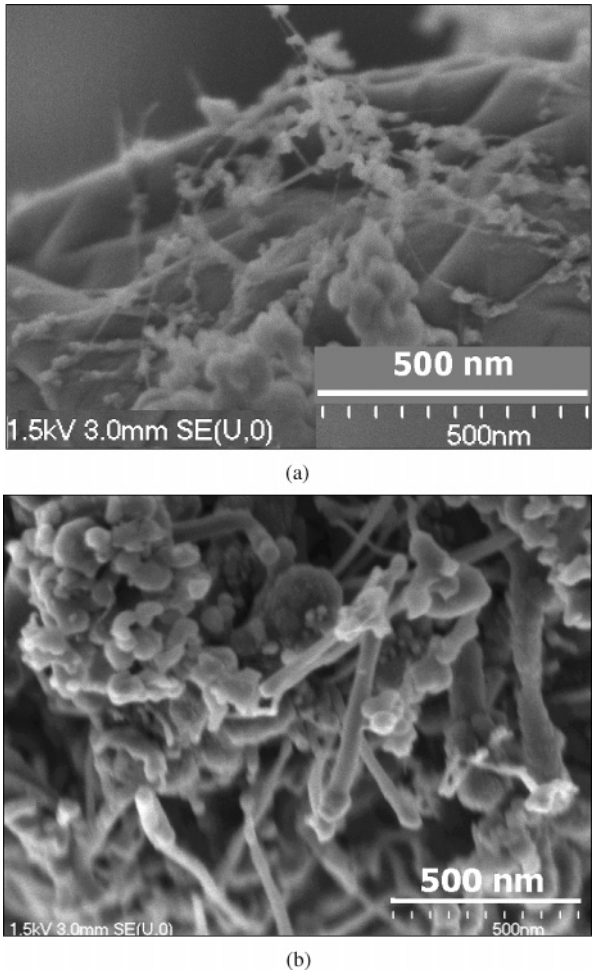

Figure 9. SEM micrographs of soot recovered from the reactor in test 5.

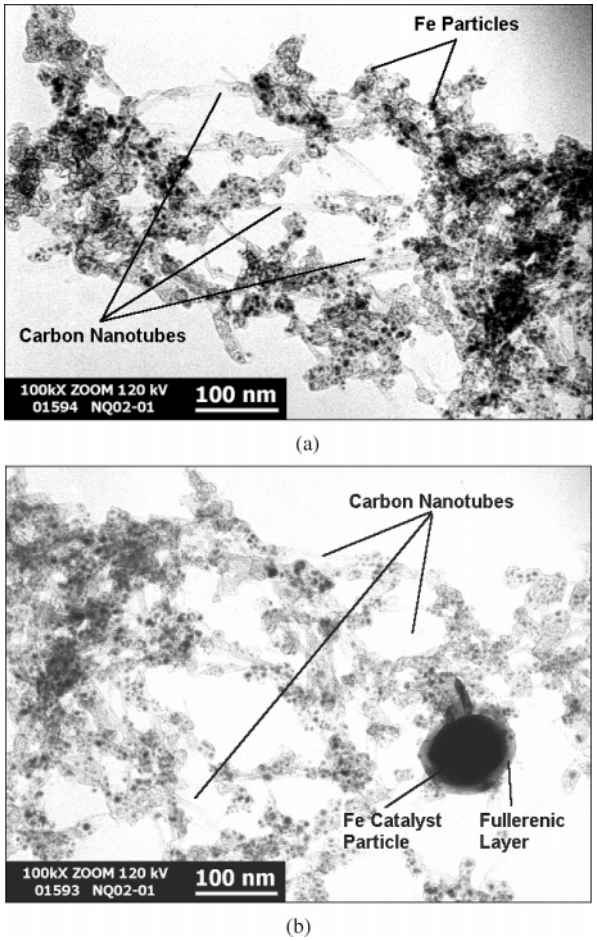

Figure 10. TEM micrographs of soot recovered from the reactor in test no. 5.

tail. The nanofiber diameters, inferred from the SEM images, range from 20 to 50 nm.

Figure 9a,b shows typical SEM images of the soot recovered from the reactor walls (Test No. 5). A high density of CNTs, with a wide diameter distribution ranging from 5 to 50 nm, can be clearly observed. Here, it is also thought that the vaporization phenomenon of the starting mixture plays an important role in the synthesis of nanotubes. An effective vaporization produces fine clusters of a catalyst and the growth of thin nanotubes might be enhanced, as shown in Figure 9a.

In contrast, the large diameters of the elongated structures depicted in Figure 9b suggest the formation of nanofibers rather than nanotubes. It can be seen that these carbon structures present a catalyst particle attached at the tip suggesting an open-ended growth mechanism, as proposed by Rao et al.[31] The high concentration of CNTs and elongated structures observed in theses images confirms the view that an efficient vaporization of reactants produces small catalyst particles, which play a key role during the growth of CNTs.

Interestingly, the nanotubes were mainly found in the soot recovered from the upper part of the reactor section. Quite low concentrations of nanotubes could be identified in the soot collected from the filter section. This latter finding suggests that the formation of nanotubes is favored by the influence of the highest temperatures and the highest carbon vapor pressures, which are present in this reactor zone.

Figure 10a,b shows TEM images of the product collected from the reactor walls in Test No. 5. Taking into account that all SEM (Figure 9) and TEM (Figure 10) images were taken from samples of the same experiment (Test No. 5), it is assumed that the elongated structures shown in Figure 9 (especially those of part a) might correspond to the nanotubes depicted in Figure 10.

The high density of nanometric iron particles indicates quite good vaporization of the reactants, which produces a sufficient concentration of carbon vapor and generates catalyst particles of smaller size within the plasma tail. Both the higher carbon vapor concentrations and the smaller catalyst particle size enhance the formation of thin carbon nanotubes. The outer diameter of the nanotubes, inferred from TEM images, ranges from 5 to 20 nm, with some nanotubes being covered by a thin layer of amorphous carbon. Figure 10b also shows an iron catalyst particle encapsulated by "fullerene-like" layers. These layers are considered to be polyaromatic sheets (hexagonal), while the curved junctions are considered to be the locations of pentagonal rings, which are characteristic of fullerene structures.

5. Conclusions

Fullerenes and nanotubes were successfully synthesized in a rf plasma reactor operated in a continuous mode of operation. A new kinetic mechanism was developed to evaluate the chemical kinetics behavior of those carbon species involved in the mechanism of fullerenes formation. This mechanism considers the fullerene growth pathway as a sequential addition of C_2 and C_3 molecules. It was shown that both the residence time and the temperature history of the growing fullerene species

play key roles in the C_{60} formation. Therefore, the experimental results confirm the validity of this kinetic mechanism. The enhancement of fullerene production was clearly observed by the presence of the iron catalyst, which also promoted the growth of CNTs. The latter were mainly formed in those reactor zones where the higher temperatures and higher carbon vapor pressures existed. Thus, it can be concluded that both the size of carbon and catalyst particles and the carbon/catalyst vapor ratio play distinctly important roles in the generation of both fullerenes and carbon nanotubes.

Acknowledgment. This work was supported by the Quebec University Network in Nanoscience and Nanotechnology (NANOQUEBEC), the Natural Science and Engineering Research Council (NSERC) of Canada, the National Council of Science and Technology (CONACYT) of Mexico, and the Committee for Scientific Research (KBN) of Poland (Grant Nr 4 TO8D 021 23). The authors also thank Irene Levesque and Pierre Magny for their technical support in performing the microscopic analyses.

References and Notes

(1) Singh, H.; Srivastava, M. *Energy Sources* **1995**, *17*, 615.
(2) Journet, C.; Bernier, P. *Appl. Phys. A* **1998**, *67*, 1.
(3) Bogdanov, A.; Deininger, D.; Dyuzhev, G. *Technol. Phys*. **2000**, *45*, 521.
(4) Churilov, G. *Inst. Exp. Technol*. **2000**, *43*, 1.
(5) Hatta, N.; Murata, K. *Chem. Phys. Lett*. **1994**, *217*, 398.
(6) Alexakis, T.; Tsantrizos, P. *Appl. Phys. Lett*. **1997**, *70*, 2102.
(7) Harbec, D.; Meunier, J. L.; Guo, L.; Gauvin, R. *Proc. 16th Int. Symp. Plasma Chem*. **2003**, 540.
(8) Peters, G.; Jansen, M. *Angew. Chem., Int. Ed. Engl*. **1992**, *31*, 223.
(9) Jansen, M.; Peters, G.; Wagner, N. *Z. Anorg. Allg. Chem.* **1995**, *621*, 689.
(10) Yoshie, K.; Kasuya, S.; Eguchi, K.; Yoshida, T. *Appl. Phys. Lett*. **1992**, *23*, 2782.
(11) Wang, C.; Imahori, T.; Tanaka, Y.; Sakuta, T.; Takikawa, H.; Matsuo, H. *Thin Solid Films* **2001**, *390*, 31.
(12) Wang, C.; Imahori, T.; Tanaka, Y.; Sakuta, T.; Takikawa, H.; Matsuo, H. *Thin Solid Films* **2002**, *407*, 72.
(13) Wang, C.; Inazaki, T.; Shirai, Y.; Tanaka, Y.; Sakuta, T.; Takikawa, H.; Matsuo, H. *Thin Solid Films* **2003**, *425*, 41.
(14) Todorovic-Markovic, B.; Markovic, Z.; Mohai, I.; Karoly, Z.; Gal, L.; Foglen, K.; Szabo, P. T.; Szepvolgyi, J. *Chem. Phys. Lett*. **2003**, *378*, 434.
(15) Cota-Sanchez, G.; Soucy, G.; Huczko, A.; Lange, H. *Trans. Mater. Res. Soc. Jpn.* **2004**, *29*, 549.
(16) Cota-Sanchez, G. Synthesis of Carbon Nanostructures Using a High Frequency Plasma Reactor, Ph.D. thesis, Sherbrooke, Qc, Canada, Université de Sherbrooke, 2003.
(17) Sekiguchi, H.; Honda, T.; Kanzawa, A. *Plasma Chem. Plasma Proc.* **1993**, *13*, 463.
(18) Coulibaly, K.; Genet, F.; Renou-Gonnord, M. F.; Amouroux, J. *High Temp. Mater. Proc*. **1997**, *1*, 473.
(19) Kee, R.; Rupley, F.; Meeks, E.; Miller, J. Sandia Natl. Lab. Sand96-8216, 1996. Livermore, CA, U.S.A.
(20) Chemical Kinetic Simulator, Version 1.0; User's Manual, IBM Corporation, IBM Almaden Research Center, 1995.
(21) Gillespie, D. *J. Phys. Chem*. **1977**, *81*, 2340.
(22) Smith, P.; Smoot, D. *Combust. Sci. Technol*. **1980**, *23*, 17.
(23) Wagner, H.; Vlasov, P.; Dorge, K.; Eremin, A.; Zaslonko, I.; Tanke, D. *Kinet. Catal*. **2001**, *42*, 583.
(24) FACTSAGE Database; Thermodynamic Equilibrium Software, version 5.0, Center for Research in Computational Thermochemistry of the Ecole Polythechnique at the Université de Montréal and GTT-Technologies, GmbH: Aachen, Germany, 2001.
(25) Duff, R.; Bauer, S. *J. Chem. Phys*. **1962**, *36*, 1754.
(26) Diky, V. V.; Kabo, G. *J. Russ. Chem. Rev*. **2000**, *69*, 95.
(27) Huczko, A.; Lange, H.; Sogabe, T. *J Phys. Chem. A* **2000**, *104*, 10708.
(28) Boulos, M.; Fauchais, P.; Pfender, E. *Thermal Plasmas. Fundamentals and Applications*; Plenum Press: New York, 1994; Vol. 1.
(29) Arbogast, J.; Darmanyan, A.; Foote, C.; Rubin, Y.; Diederich, F.; Alvarez, M.; Anz, S.; Whetten, R. *J. Phys. Chem*. **1991**, *95*, 11.
(30) Chibante, L.; Andreas, T.; Alford, J.; Diener, M.; Smalley, R. *J. Phys. Chem*. **1993**, *97*, 8696.
(31) Rao, C.; Satishkumar, B.; Govindaraj, A.; Nath, M. *ChemPhysChem* **2001**, *2*, 78.